

## MONONUCLEAR ACTIVE SITES OF MOLYBDOENZYMES: CHEMICAL APPROACHES TO STRUCTURE AND REACTIVITY

R. H. Holm and Jeremy M. Berg

Department of Chemistry, Harvard University, Cambridge, Massachusetts,  
USA 02138

**Abstract** - One of two general classes of molybdoenzymes contains mononuclear catalytic sites and effects oxidation or reduction of substrate X/XO by oxygen atom transfer:  $X + (O) \rightleftharpoons XO$ . The reaction  $L_n MoO_2 + X \rightarrow L_n MoO + XO$  is well established in synthetic systems, and is frequently accompanied by dimerization of Mo(VI,IV) complexes to  $[L_n Mo(V)-O]_2O$ . A general kinetic analysis allowing determination of oxo-transfer rate constants in systems with  $\mu$ -oxo dimer formation is outlined. EXAFS results for several enzymes indicate the minimal coordination spheres  $Mo(VI)O_2(SR)_{2,3}$  and  $Mo(IV)O(SR)_{3,4}$  for oxidized and fully reduced forms, respectively. In a synthetic approach to these sites, the ligand pyridine-2,6-bis(1,1-diphenylethanethiol) ( $L-N(SH)_2$ ) was prepared. Reaction with  $MoO_2(acac)_2$  afforded the 5-coordinate trigonal bipyramidal complex  $MoO_2(L-NS_2)$ , which was converted to  $MoO(L-NS_2)(DMF)$  with  $Ph_3P$  in DMF. In this and other oxo-transfer reactions of these complexes, the gem-diphenyl groups sterically suppress dimerization to a  $Mo(V)-O-Mo(V)O$  complex. This reaction is blocked in enzymes by protein structural constraints.  $MoO(L-NS_2)(DMF)$  and  $Me_2SO$  react to produce  $MoO_2(L-NS_2)$  and  $Me_2S$ . Substrate saturation kinetics are observed at sufficient  $Me_2SO$  concentrations. The two reactions were coupled to generate a catalytic sulfoxide reduction/phosphine oxidation cycle. In a related reaction, d-biotin-d-sulfoxide is reduced by  $MoO(L-NS_2)(DMF)$  to d-biotin. Inasmuch as d-biotin-d-sulfoxide reductase is a Mo cofactor-dependent enzyme, this reaction provides a meaningful model for an enzymatic oxo-transfer reaction. Kinetic data for various oxo-transfer reactions are presented and their relevance to enzymatic processes is discussed.

### INTRODUCTION

Molybdenum-containing enzymes are of two types: nitrogenases (1-6), which catalyze the reduction of dinitrogen to ammonia, and oxo-transfer enzymes (2,3,7,8), which catalyze what is in effect the transfer of oxygen atoms from or to the substrates X/XO. The latter transformations may be written most simply as reaction [1] or, to emphasize the two-electron nature of the overall processes, as the half-reaction [2]. Representative molybdoenzymes of



the oxo-transfer type are listed in Table 1. For sulfite oxidase and xanthine oxidase/dehydrogenase in particular, abundant evidence has demonstrated that a mononuclear Mo coordination unit is the catalytic site. In addition to this site, every enzyme that has been at least partially characterized contains one or more prosthetic groups (heme, flavin, Fe-S cluster) capable of electron storage and transfer.

Both nitrogenase and oxo-transfer molybdoenzymes contain dissociable cofactors that are obligatory for catalytic activity but which, except for containing all the molybdenum in a given enzyme, are chemically unrelated. The cofactor of nitrogenase is a Mo-Fe-S cluster of incompletely defined composition and structure (9, 10). The cofactor (Mo-co) of oxo-transfer enzymes (11) is not yet well characterized but has been shown to contain a pterin nucleus carrying a potentially coordinating side chain. Certain leading results of the Duke group (12-14) bearing on the structure of Mo-co from several enzymes are schematically illustrated in Fig. 1. Denaturation of sulfite oxidase and xanthine dehydrogenase from chicken liver and *Chlorella* nitrate reductase with 6 M guanidine HCl in the presence of KI and  $I_2$  led to dissociation of the same fluorescent species (form A). When denaturation was performed in boiling pH 2.5 solution, a different fluorescent species (form B) was released. The permanganate

TABLE 1. Representative oxo-transfer molybdoenzymes

Enzyme/Source	M <sub>r</sub>	Subunits	Mo Content	Prosthetic Groups
Sulfite Oxidase rat liver	114,000	α <sub>2</sub>	2	heme
Xanthine Oxidase bovine milk	275,000	α <sub>2</sub>	2	FAD, 4Fe <sub>2</sub> S <sub>2</sub>
Xanthine Dehydrogenase rat liver	280,000	α <sub>2</sub>	2	FAD, 4Fe <sub>2</sub> S <sub>2</sub>
Nitrate Reductase <i>E. coli</i>	200,000	αβ	1	Fe-S
Nitrate Reductase spinach	197,000	α <sub>2</sub> β <sub>2</sub>	1	heme, FAD
CO Methylene Blue Oxidoreductase <i>Ps. carboxydovorans</i>	230,000	α <sub>2</sub>	2	Fe-S, FAD
CO Ferredoxin Oxidoreductase <i>C. pasteurianum</i>	118,000	αβ	1	Fe-S
Formate Dehydrogenase <i>Methanobacterium formicicum</i>	288,000	unknown	2	Fe-S
Biotin Sulfoxide Reductase <i>E. coli</i>	unknown	unknown	present	unknown
Pyridoxal Oxidase <i>Drosophila melanogaster</i>	unknown	unknown	present	unknown

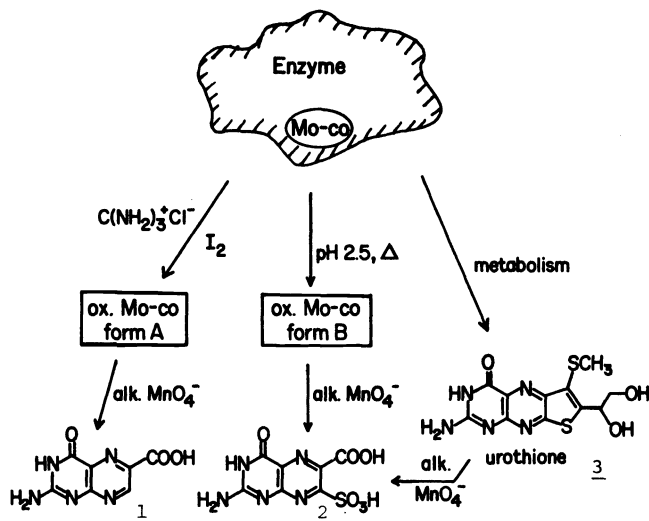
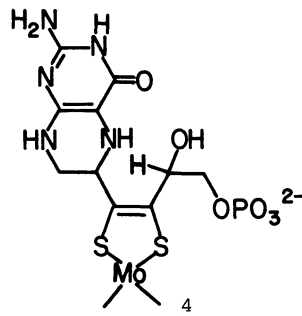


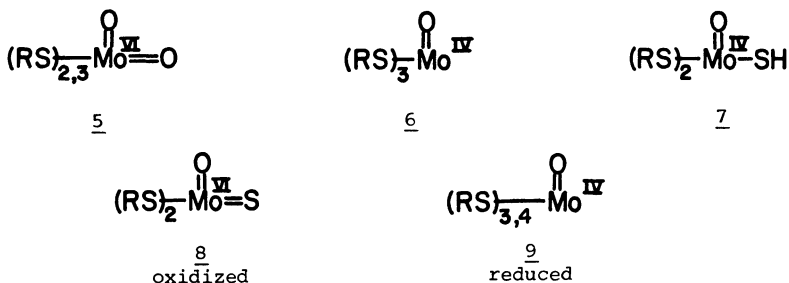
Fig. 1. Removal and oxidation of Mo-co from chicken liver sulfite oxidase and other enzymes (13).

oxidation products of these forms were identified as pterin-6-carboxylic acid (1) and pterin-6-carboxylic-7-sulfonic acid (2). Oxidation of urothione (3) also afforded 2, indicating a structural relationship between form B and 3. Prior to oxidation form B was shown to possess a terminal phosphate group, which was removable with alkaline phosphatase to form a glycol. The finding that persons deficient in Mo-co are devoid of 3 in urine samples provides a metabolic link between the cofactor and urothione. On the basis of these and other observations, including the presence of two sulfur atoms in 3 and the detection of Mo-S ligation from EXAFS analysis, the partial structure 4 of the active form of Mo-co was proposed (13). Because all observations leading to



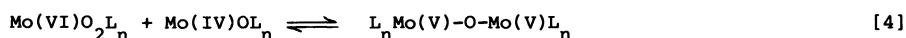
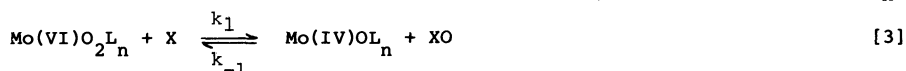
this proposal were made under oxidizing conditions, the tetrahydropterin nucleus of 4 was not observed. It and the 1,2-dithiolene structure in the side chain are conjectural.

The most incisive information concerning Mo-ligand interactions derives from the analysis of Mo EXAFS. The principal results of Cramer *et al.* (15,16) for oxidized and reduced sulfite oxidase (5, 6), xanthine dehydrogenase (7, 8), and *Chlorella* nitrate reductase (5, 9) are



shown in the form of those atoms most securely identified by the technique. Other ligands, especially those with lower atomic number (N, O), are presumably present. Common to all sites are multiply-bonded oxo atoms at  $\sim 1.7 \text{ \AA}$  from the Mo(IV,VI) atoms. A terminal sulfido ligand of the type in 8 has been detected by EXAFS in the oxidized form of bovine xanthine oxidase (17). Its presence is also indicated by chemical and spectroscopic properties of the enzyme. The Mo(VI,IV)-S distances of  $\sim 2.4 \text{ \AA}$  in 5-9 are consistent with thiolate rather than thioether ligation. All of these results were obtained on holoenzymes. It is not yet known what structural features detectable in EXAFS spectra are common to the Mo coordination unit in the native enzymes and in Mo-co. The existence of a cofactor was first suggested by genetic results obtained in 1964 (18). The proposition of a common cofactor was placed on firm grounds by the work of Nason *et al.* (19), who demonstrated activation of nitrate reductase from *Neurospora crassa* mutant *nit-1* by addition of extracts of the wild type organism and other molybdoenzymes whose cofactors are dissociated by acid treatment. Subsequent significant observations include reconstitution of demolybdo sulfite oxidase obtained from the livers of tungsten-fed rats by the same sources of cofactor active in the *Neurospora nit-1* systems (20); and the absence of cross-complementary activation of *nit-1* nitrate reductase and an inactive nitrogenase from a mutant strain of *Azotobacter vinelandii* by the cofactors of nitrate reductase and xanthine oxidase, and the nitrogenase cofactor (21). The ability to reconstitute to full activity cofactor-deficient enzymes by extracts from active forms of the same and different oxo-transfer enzymes (14) strongly implies a common structure of at least the organic component binding the Mo atom in Mo-co. However, given the EXAFS determinations of the minimal coordination units 5-9 of different enzymes, it appears that all features of these units are not conserved.

We have undertaken an investigation whose goal is the simulation of stoichiometric or catalytic reactions of the enzymes in Table 1 using credible synthetic representations of their Mo sites. These sites must, *inter alia*, (i) approach or duplicate the native ligand set, (ii) execute the forward or reverse reaction [3] with substrate X/XO, and (iii) not undergo the  $\mu$ -oxo dimerization reaction [4]. To satisfy requirement (i), the ligand set  $L_n$  must



contain at least two thiolate ligands. Requirement (ii) is offered in terms of the overall reaction [3], with the allowance that the oxygen atom actually transferred may derive from solvent water. Reaction [4] is prevented by protein structural constraints, thereby leading to requirement (iii). Further, if dimerization is irreversible in model systems, even stoichiometric conversion of substrate in reaction [3] is precluded provided the two reactions have competitive rates. While a number of interesting structural models of enzyme sites, especially those containing the  $\text{MoO}_2$  unit, have been prepared (22-28), none satisfies requirements (i)-(iii) simultaneously. We describe here some of our initial results on biologically relevant oxo-transfer reactions with Mo(VI,IV)-oxo-thiolate complexes (29).

#### FORMATION OF $\mu$ -OXO MOLYBDENUM(V) COMPLEXES

The dimerization reaction [4] is a pervasive feature of synthetic molybdenum chemistry. Many examples of irreversible and reversible reactions have been described. In addition to their deleterious effect on substrate oxidation or reduction, irreversible reactions prevent the synthesis of  $\text{MoOL}_n$  complexes by the frequently employed method of oxo atom abstraction from  $\text{MoO}_2L_n$  species with oxophilic reagents. Reversible reactions do not necessarily prevent substrate transformation or synthesis of Mo(IV) complexes but, as already noted, they are not

realistic components of a model enzymatic reaction system. There being no assurance at the outset that systems lacking this reaction could be achieved, a kinetics analysis allowing abstraction of the rate constant  $k_1$  or  $k_{-1}$  of an irreversible reaction [3] in the presence of a reversible reaction [4] was developed (30). Prior kinetics treatments of this problem have been inadequate in scope and accuracy.

The prototype system selected for investigation was composed of reactions [5] and [6] ( $R = Ph$ ,  $L = Et_2NCS_2^-$ ), whose occurrence had been well documented (31,32). The kinetics treatment



has as its only assumption equilibrium of the dimerization reaction at all points along the oxo transfer reaction coordinate. Under this assumption the rate law is given by eq. [7], where  $dx$  is the infinitesimal concentration change along the oxo transfer coordinate,  $dy$  is

$$\begin{aligned} \frac{d[MoO_2L_2]}{dt} &= -k_1[MoO_2L_2][R_3P](1 + dy/dx) \\ &= k_1 \frac{[MoO_2L_2](K + 2[MoO_2L_2])([MoO_2L_2]^2 + (K + 2P - C)[MoO_2L_2] + K(P - C))}{2[MoO_2L_2]^2 + 2K[MoO_2L_2] + K^2 + CK} \quad [7] \end{aligned}$$

the corresponding change in the dimerization reaction to maintain equilibrium,  $P = [R_3P]$ , and  $C$  is the total concentration of Mo in all forms. Separation of variables and integration affords the integrated rate law given in functional form as eq. [8]; the explicit expression is available elsewhere (30). Rate constants evaluated from fits of absorbance data to the

$$-k_1 t = f([MoO_2L_2]_t, K, C, P) \quad [8]$$

rate law are given in Table 2. Values of  $k_1$  monotonically increase with increasing phosphine nucleophilicity. In this system the  $\mu$ -oxo dimer is extensively dissociated. The forward and

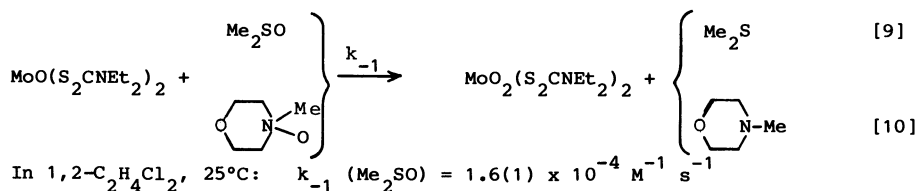
TABLE 2. Kinetic and equilibrium data for reactions [3] and [4] ( $L = Et_2NCS_2^-$ ) in 1,2-dichloroethane at 25°C

Substrate	$k_1$ ( $M^{-1}s^{-1}$ ) <sup>a</sup>
PEt <sub>3</sub>	0.53(1)
PPhEt <sub>2</sub>	0.43(2)
PPh <sub>2</sub> Et	0.23(2)
PPh <sub>3</sub>	0.071(3)
PPh <sub>3</sub>	$K = 0.0017 M^a$ , $0.0020 M^b$
	$k_2 = 2.93 s^{-1}$ , $k_{-2} = 1470 M^{-1}s^{-1} b$

<sup>a</sup>Ref. 30. <sup>b</sup>Ref. 32.

reverse rate constants of reaction [6], measured by the temperature jump method (32), correspond to appreciable rates in both directions. These and the excellent agreement between experimental absorbance vs. time behavior and that calculated from the theoretical rate law demonstrate the validity of the treatment.

In further experiments it was determined spectrophotometrically that  $MoO(S_2CNET_2)_2$  in  $Me_2SO$  was oxidized to  $MoO_2(S_2CNET_2)_2$  in reaction [9], consistent with an earlier visual observation (33). This reaction, which is an example of the reverse of reaction [3], is rather slow.

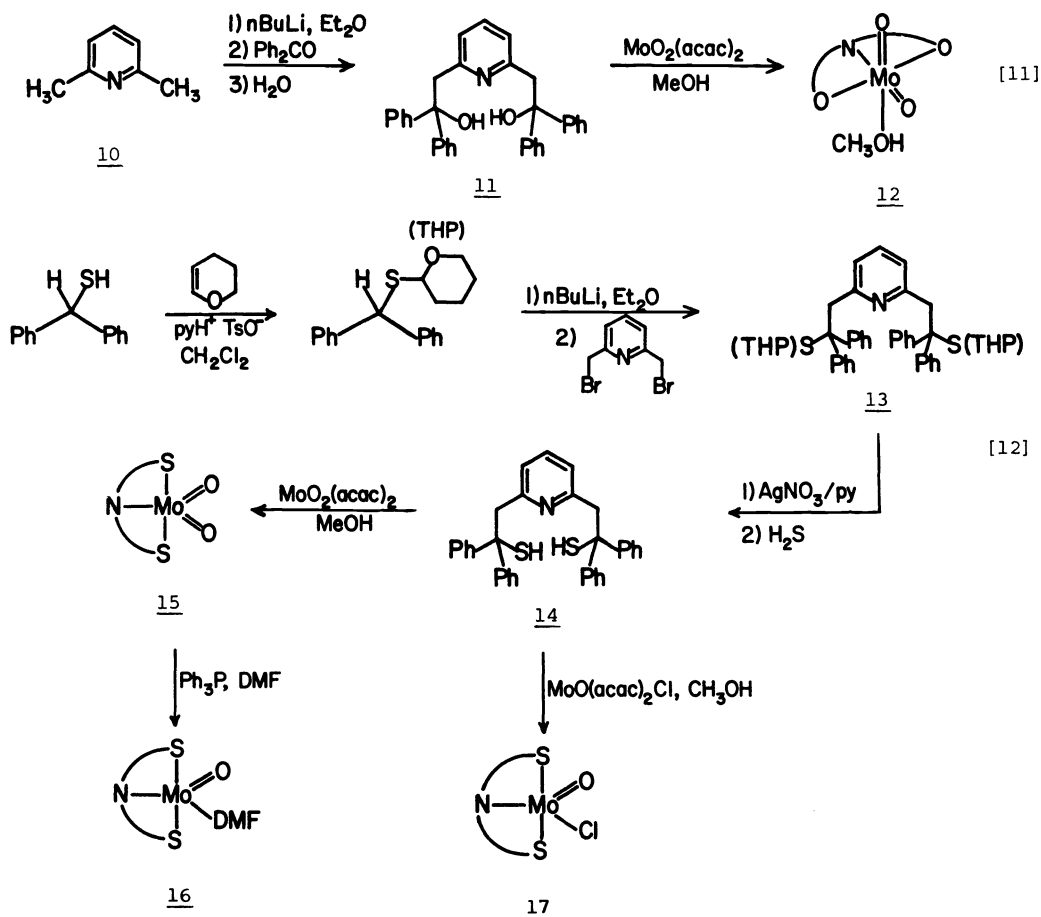


The indicated rate constant, obtained by the same kinetics analysis (30), is several orders of magnitude less than those for phosphine oxidation. With N-methylmorpholine-N-oxide, the

rate of reaction [10] is orders of magnitude faster, suggesting that breaking of the bond to oxygen is the most important factor (in the absence of steric effects) in governing oxo atom transfer to the Mo(IV) reactant. These results demonstrate oxo transfer to and from substrate and show that rate constants for these processes can be abstracted from systems consisting of the coupled reactions [3] and [4], so long as the latter is reversible and equilibrates quickly. However, reaction systems lacking the dimerization equilibrium are far more convenient to examine and, as already emphasized, are the more biologically realistic. Their development constituted the next phase of the investigation.

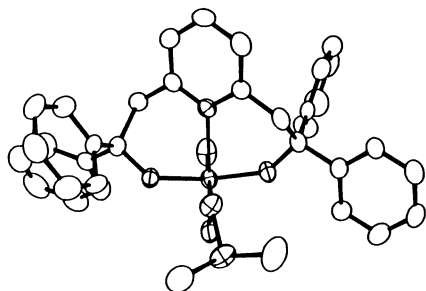
#### STERICALLY HINDERED MONONUCLEAR MOLYBDENUM(VI, IV) COMPLEXES

**Synthesis.** Suppression of the dimerization reaction [4] by steric constraints was examined in the form of the products of synthetic schemes [11] and [12]. Dilithiation of 2,6-lutidine (10) followed by reaction with benzophenone and hydrolysis gave the diol 11 (L-N(OH)<sub>2</sub>, 36%), which with MoO<sub>2</sub>(acac)<sub>2</sub> yielded the colorless complex 12 (MoO<sub>2</sub>(L-NO<sub>2</sub>)(MeOH), 90%). S-protection of diphenylmethanethiol, lithiation, and reaction with bis(2,6-bromomethyl)pyridine afforded the protected dithiol 13 (82%). Deprotection of this compound produced the sensitive dithiol 14 (L-N(SH)<sub>2</sub>), which with MoO<sub>2</sub>(acac)<sub>2</sub> smoothly formed the orange Mo(VI) complex 15 (MoO<sub>2</sub>(L-NS<sub>2</sub>), 85%). Treatment of 15 with Ph<sub>3</sub>P in DMF yielded the purple Mo(IV) complex 16 (MoO(L-NS<sub>2</sub>)(DMF)). The brown Mo(V) complex 17 was obtained by the reaction of 14 with MoO(acac)<sub>2</sub>Cl in methyl alcohol. At this stage of development of the problem, the two thiolate ligands in the complexes of 14 provide a reasonable solution to the requirement (i). Ligands 11 and 14 carry bulky gem-diphenyl substituents next to coordinating oxygen and sulfur atoms, respectively, in an attempt to prevent dimerization by steric hindrance.



**Structures.** When recrystallized from Me<sub>2</sub>SO, MoO<sub>2</sub>(L-NO<sub>2</sub>) is obtained as its Me<sub>2</sub>SO adduct **18**, whose structure has been determined by X-ray analysis. Mean dimensions are indicated. MoO<sub>2</sub>(L-NO<sub>2</sub>)(Me<sub>2</sub>SO) has distorted octahedral stereochemistry with cis oxo and trans alkoxide ligands; Me<sub>2</sub>SO is coordinated through its oxygen atom. Overall, the stereo-

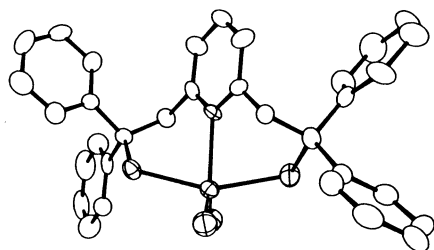
chemistry is rather similar to those of other six-coordinate  $\text{MoO}_2$  complexes (23-25,34). The



18

Mo-O	1.705 Å		
Mo-O (C)	1.902		
Mo-O (S)	2.382		
Mo-N	2.417		
O-Mo-O	105.4°	O (C)-Mo-O (C)	153.2°
O-Mo-O (C)	96.8°	O-Mo-N	166.3°
N-Mo-O (C)	81.7°	O-Mo-O (S)	167.6°

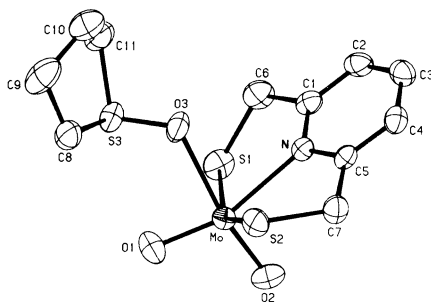
structure of  $\text{MoO}_2(\text{L-NS}_2)$  is quite different and provides a new stereochemical type of dioxo-Mo(VI) complex. The five-coordinate  $\text{MoO}_2\text{NS}_2$  unit is a distorted trigonal bipyramid with a



15

Mo-O	1.694 Å		
Mo-S	2.416		
Mo-N	2.244		
O-Mo-O	110.5°	S-Mo-S	156.4°
O-Mo-S	95.2°	O-Mo-N	126.4°
N-Mo-S	78.4°		

$\text{MoO}_2\text{N}$  equatorial plane, axial sulfur atoms, and an idealized  $C_2$  axis along the Mo-N bond. The Mo-S distance is in the 2.41-2.47 Å range determined for oxidized enzyme sites 5 and 8 by EXAFS analysis (15,16). This distance is essentially the same (2.420 Å) in 19, a distorted octahedral complex derived from pyridine-2,6-dimethanethiol and crystallized as its tetramethylsulfoxide adduct (25). The structures of 16 (and other adducts) and 17 have not yet been determined by diffraction methods. The proposed structures are based on replacement of one oxo ligand of 15 with retention of five-coordinate geometry. The phenyl groups in 15 and 18 provide an extent of frontside hindrance to their Mo atoms, one aspect of which is the projection of their structures on the Mo=O bonds, i.e., along the direction of potential  $\mu$ -oxo bond formation.



19

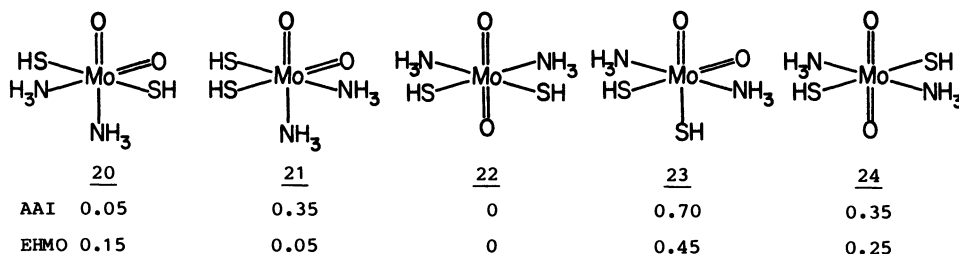
#### LIGAND SITE PREFERENCES

The distorted octahedral structure of  $\text{MoO}_2(\text{L-NO}_2)(\text{Me}_2\text{SO})$  (18) is typical of the majority of known  $\text{MoO}_2\text{X}_2\text{L}_2$  structures in which X is an anionic and L is a neutral ligand. These complexes are characterized by cis oxo atoms and trans X ligands and X-Mo=O angles somewhat greater than 90°. The reasons for the stability of this structural type raise some important issues with regard to bonding in dioxo-Mo(VI) complexes.

The universal preference for a nonlinear configuration of the  $[\text{MoO}_2]^{2+}$  group has been rationalized in terms of competition by strong  $\sigma$ - and  $\pi$ -donor oxo ligands for acceptor orbitals on the Mo atom. This has been put into quantitative terms by Tatsumi and Hoffmann (35) on the basis of extended Hückel molecular orbital (EHMO) calculations for  $[\text{MoO}_2]^{2+}$ . A plot of total energy vs. O=Mo=O angle shows a minimum at  $\sim 110^\circ$  with a depth (vs. the trans structure) of 0.6 eV. The angle of maximum stability conforms to within ca. 5° of angles in a large variety of dioxo-Mo(VI) structures. In this study EHMO calculations on other fragments have been carried out using conventional bond distances and ligand geometries. Calculations for the  $[\text{HS-Mo=O}]^{3+}$  group reveal a behavior similar to  $[\text{MoO}_2]^{2+}$ . Thiolate ligands are  $\sigma$ - and  $\pi$ -donors of strength roughly comparable to that of an oxo ligand. The calculational result could perhaps have been anticipated, for there are no known examples of a thiolate group trans to an oxo ligand. The curve for  $[\text{HS-Mo-SH}]^{4+}$  is slightly less deep (0.5 eV) while

those for  $[\text{H}_3\text{N-Mo=O}]^{4+}$ ,  $[\text{H}_3\text{N-Mo-SH}]^{5+}$ , and  $[\text{H}_3\text{N-Mo-NH}_3]^{6+}$  are substantially less deep ( $\sim 0.3$  eV), than the  $[\text{MoO}_2]^{2+}$  result. All curves have minima in the 100-115° range. The energy curves can be used to estimate the relative energies of various configurations of a dioxo-Mo(VI) complex containing thiolate and nitrogen-donor ligands. The procedure is illustrated for the  $\text{MoO}_2\text{S}_2\text{N}_2$  coordination unit, as contained in  $\text{MoO}_2(\text{SH})_2(\text{NH}_3)_2$ , a hypothetical species simplified for calculational purposes. For a given geometry the relative energy is defined to be the sum of  $6!/2!4! = 15$  angular interactions (one for each possible set of two ligands), based on the energy curves. The local minima in the energy surface specified in this manner can be found by choosing an approximately octahedral starting configuration and making small iterative corrections in the ligand positions until the energy function reaches a minimum. This approach allows a rapid evaluation of a number of different structures with as few a priori assumptions as possible. Comparison with full EHMO calculations based on the minimum energy geometries reveals that the method affords reasonable approximate relative energies.

There are five possible isomers 20-24 for octahedral  $\text{MoO}_2(\text{SH})_2(\text{NH}_3)_2$ . The relative energies



(eV) of the local minima corresponding to each, based on the additive angular interaction method (AAI), are given together with those from full EHMO calculations. The three most stable structures are 20-22. As already noted, 20 is the most commonly observed structural type (23). Structure 21 has not yet been observed in a  $\text{MoO}_2$ -thiolate complex, although two complexes with  $\text{MoO}_2(\text{OR})_2(\text{imine})_2$  coordination units possess analogous stereochemistry (36). The local minimum derived from starting configurations of 22 correspond to a severely distorted octahedral arrangement, with the  $\text{O=Mo=O}$  angle ( $\sim 160^\circ$ ) closed down substantially from  $180^\circ$ . This arrangement bears a definite resemblance to the unusual skew-trapezoidal geometry exhibited by  $\text{MoO}_2(\text{SCMe}_2\text{CH}_2\text{NHMe})_2$  and related complexes (23). The enhanced stability of 20-22 compared to 23 and 24 can be rationalized in terms of the presence of only one unfavorable trans  $\text{O=Mo=O}$ ,  $\text{HS-Mo=O}$ , or  $\text{HS-Mo-SH}$  interaction, whereas the latter two species have two such interactions.

On the basis of experimental observations, structure 20 is the most stable configuration. This is an example of the usual circumstance of weaker  $\pi$ -bonding ligands trans to oxo atoms where they are not competing for available empty d-orbitals (37). However, in systems where the thiolate ligands are constrained so that they cannot be mutually trans, structure 21 and 22 (with a bent  $\text{MoO}_2$  group) are reasonable possibilities. The suggested partial structure 4 of Mo-co contains cis thiolate ligands. If in its dioxo-Mo(VI) form the species is six-coordinate, the results of this treatment suggest that structures 21 and bent 22 are more viable configurations than 23, which contains two unfavorable  $[\text{HS-Mo=O}]^{3+}$  interactions. Conclusions as to relative stabilities of 20-24 are not significantly dependent on the choice of Mo-S-H torsional angles.

The method is readily extended to five-coordinate Mo(VI) structures of hypothetical  $\text{MoO}_2(\text{SH})_2(\text{NH}_3)$ . For this case there are  $5!/2!3! = 10$  angular interactions. There are at least six local minima in the energy surface arising from the AAI procedure. One of these corresponds to the structure of  $\text{MoO}_2(\text{L-NS}_2)$  (15), viz., a distorted trigonal bipyramid with axial thiolate ligands. Interestingly, this configuration is  $\sim 0.3$  eV higher in energy (by the AAI procedure) than another trigonal bipyramidal configuration with axial oxo and  $\text{NH}_3$  ligands, related to the preceding structure by a pseudorotation. This observation suggests that the observed structure 15 is set by chelate ligand constraints that place the sulfur atoms in axial positions, at a S-Mo-S angle of  $156.4^\circ$ .

#### REACTIVITIES OF COMPLEXES 15 AND 16

Oxo Transfer to Substrate. The propensity of  $\text{MoO}_2(\text{L-NS}_2)$  (15) to transfer an oxygen atom to substrate was examined in systems containing  $\text{Ph}_3\text{P}$  in DMF. Spectral changes pursuant to the reaction in one such system are shown in Fig. 2. The initial complex has bands at 385 ( $\epsilon_M$  4400) and 449 (3900) nm. These are thiolate LMCT absorptions and are possibly related to the features at 350 and  $\sim 475$  nm in the spectrum of the isolated Mo domain of sulfite oxidase (38). Few spectra of dioxo-Mo(VI) thiolate complexes have been reported; those of, e.g.,

$\text{MoO}_2(\text{L-Cys}\cdot\text{OR})_2$  have maxima at  $\sim 350$  ( $\epsilon_M \sim 5000$ ) nm (39). In the reaction isosbestic points

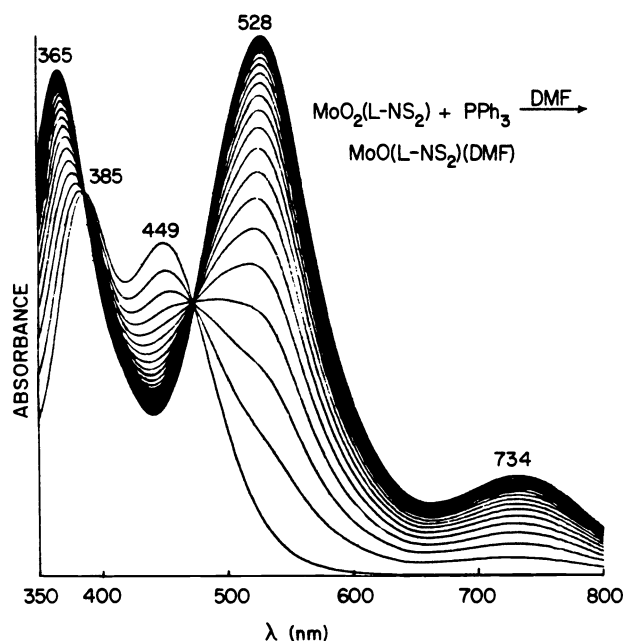
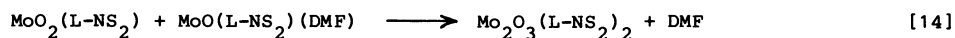
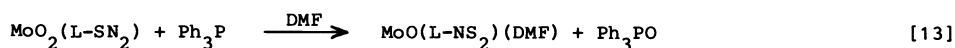


Fig. 2. Spectral changes in the reaction of 0.1 mM 15 and 3 equivalents of  $\text{Ph}_3\text{P}$  in DMF solution at 23°C.

are developed at 386 and 473 nm, indicating the formation of a single product which could arise from reaction [13] alone or coupled with reaction [14]. The stoichiometries of reaction [13] and reactions [13] + [14] differ, and were experimentally distinguished by treatment of 10 mM  $\text{MoO}_2(\text{L-NS}_2)$  with 1.88 equivalents of  $\text{Ph}_3\text{P}$  in DMF and examination of the  $^{31}\text{P}$  NMR



spectrum after completion of reaction. Signals at -4.6 ( $\text{Ph}_3\text{P}$ ), 25.9 ( $\text{Ph}_3\text{PO}$ ), and 43.5 ppm vs. 85%  $\text{H}_3\text{PO}_4$  (external) were observed. The last signal was assigned to  $\text{MoO}(\text{L-NS}_2)(\text{OPPh}_3)$ . Relative signal intensities were consistent only with reaction [13], in which 1 equivalent of  $\text{Ph}_3\text{P}/\text{Mo}$  is consumed. Further, the final absorption spectrum is identical to that of  $\text{MoO}(\text{L-NS}_2)(\text{DMF})$  (16) isolated in Scheme [12]. These results unequivocally demonstrate the absence of a  $\mu$ -oxo dimer product. In 1,2- $\text{C}_2\text{H}_4\text{Cl}_2$  solution complex 19 reacts with  $\text{Ph}_3\text{P}$  to yield a brown, sparingly soluble solid ( $\nu_{\text{MoO}}$  945, 790  $\text{cm}^{-1}$ ). The same product results from the reaction of pyridine-2,6-dimethanethiol with  $\text{Mo}_2\text{O}_3(\text{acac})_4$ . By its method of synthesis this product is identified as the  $\mu$ -oxo dimer  $\text{Mo}_2\text{O}_3(\text{C}_5\text{H}_3\text{N-2,6-(CH}_2\text{S)}_2)_2$ . The formation of this species stands in strong contrast to the outcome of reaction [13]. The gem-diphenyl groups of 15 evidently provide the intended steric suppression of  $\mu$ -oxo dimer formation, affording in this sense a more biologically realistic oxo-transfer reactant. As will be seen, the same behavior holds in oxo-transfer processes of complex 16.

Reaction [13] conforms to the rate law [15]. At 23°C  $k = 7(1) \times 10^{-3} \text{ M}^{-1} \text{ s}^{-1}$ , a value ten times smaller than the rate constant for the reaction of  $\text{MoO}_2(\text{S}_2\text{CNET}_2)_2$  with the same phosphine in 1,2- $\text{C}_2\text{H}_4\text{Cl}_2$  (Table 2). It is an order of magnitude larger than the rate constants

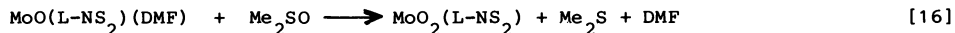
$$\frac{d[\text{MoO}_2(\text{L-NS}_2)]}{dt} = -k[\text{MoO}_2(\text{L-NS}_2)][\text{Ph}_3\text{P}] \quad [15]$$

for the more reactive  $\text{Ph}_2\text{PEt}$  with a series of  $\text{MoO}_2$  complexes containing tridentate salicylaldimino ligands with one coordinated thiolate (40). Formation of  $\mu$ -oxo dimers apparently does not intervene in these systems, whose rate constants increase with increasing potentials  $E_{p,c}$  for irreversible reduction of the Mo(VI) reactants. The latter observation is consistent with our finding that, while 15 ( $E_{p,c} = -0.89$  vs. SCE) readily reacts with  $\text{Ph}_3\text{P}$ , 18 ( $E_{p,c} = -1.82$  V) is inert. Here, and generally, thiolate ligands have the property of increasing Mo reduction potentials, signifying more easily reduced species and leading to



increased reaction rates.

**Oxo Transfer from Substrate.** Documented (non-enzymatic) examples of the reverse of reaction [3], wherein substrate is reduced and Mo is oxidized, are rare. Reactions [9] and [10] effect substrate reduction and led to an examination of reaction [16], which is readily monitored spectrophotometrically. Spectral changes are the reverse of those in Fig. 2, with the



365 and 528 nm bands decreasing, and the 449 nm band increasing, in intensity as the reaction proceeds. Analogous isosbestic points are observed. Reaction [16] shows remarkable kinetic behavior. At sufficient levels of  $\text{Me}_2\text{SO}$  the rate is independent of substrate concentration. The rate dependence on  $\text{Me}_2\text{SO}$  concentration is shown in Fig. 3. The saturation effect is

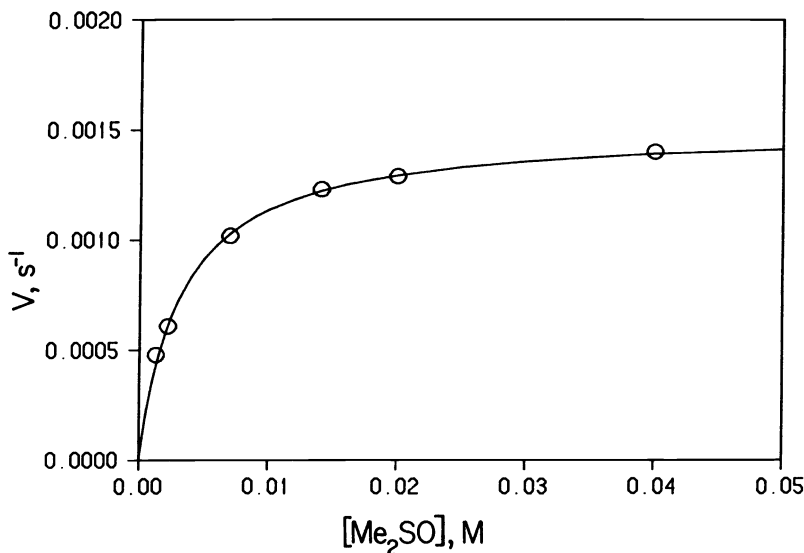
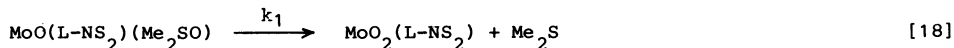
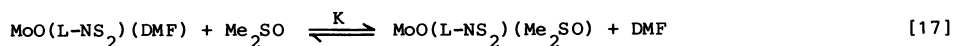


Fig. 3. The effect of  $\text{Me}_2\text{SO}$  concentration on the rate of disappearance of  $\text{MoO}(\text{L-NS}_2)\text{Y}$ . The curve is calculated from eq. [19] using  $k_1$  and  $K$  values in the text.

analogous to frequently observed enzymatic behavior and, as in such cases, it arises from substrate binding prior to conversion to product. The situation is described by reactions [17] and [18]. The rate law, expressed in terms of the disappearance of the combined Mo(IV)



species  $\text{MoO}(\text{L-NS}_2)\text{Y}$ , is given by eq. [19], where the quotient represents the fraction of

$$\begin{aligned} \frac{d[\text{MoO}(\text{L-NS}_2)\text{Y}]}{dt} &= -k_1 [\text{MoO}(\text{L-NS}_2)(\text{Me}_2\text{SO})] \\ &= -k_1 \left( \frac{K[\text{Me}_2\text{SO}]}{K[\text{Me}_2\text{SO}] + [\text{DMF}]} \right) [\text{MoO}(\text{L-NS}_2)\text{Y}] \end{aligned} \quad [19]$$

Mo(IV) species present as the  $\text{Me}_2\text{SO}$  adduct. The reaction rate is then expressible by eq. [20]. A double reciprocal plot of  $1/V$  vs.  $1/[\text{Me}_2\text{SO}]$ , entirely analogous to a Lineweaver-Burk plot used in enzyme kinetics analysis, has the form of eq. [21]. From the plot in Fig. 4,

$$v = k_1 \left( \frac{K[\text{Me}_2\text{SO}]}{K[\text{Me}_2\text{SO}] + [\text{DMF}]} \right) \quad [20]$$

$$\frac{1}{v} = \frac{1}{k_1} + \frac{[\text{DMF}]}{k_1 K} \frac{1}{[\text{Me}_2\text{SO}]} \quad [21]$$

$k_1 = 1.5 \times 10^{-3} \text{ s}^{-1}$ , corresponding to the maximum reaction velocity, and  $K = 4 \times 10^3$ , reflecting the stronger binding of  $\text{Me}_2\text{SO}$  over DMF in DMF solution. Kinetic parameters for the reduction of  $\text{Ph}_2\text{SO}$  in DMF solution are quite similar to those for  $\text{Me}_2\text{SO}$ .

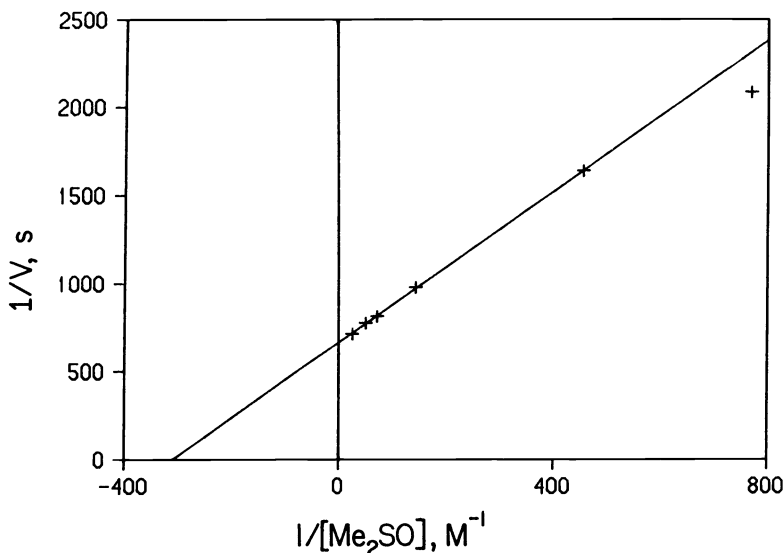
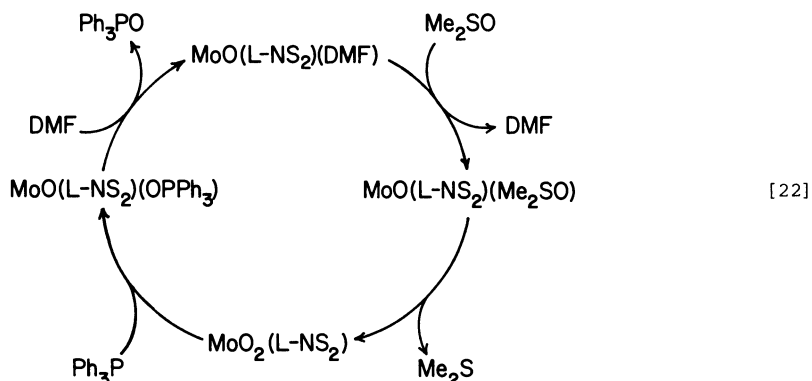
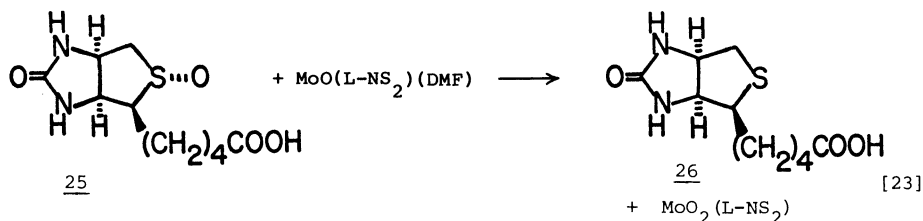


Fig. 4. A double reciprocal plot of the data in Fig. 3. The line is calculated from eq. [21] with  $k_1$  and  $K$  values given in the text.

**Catalysis.** Reactions [13] and [16], involving oxidation of  $\text{Ph}_3\text{P}$  and reduction of  $\text{Me}_2\text{SO}$ , respectively, may be coupled to form a catalytic system which is operable at ambient temperature. In one experiment  $\text{MoO}_2(\text{L-NS}_2)$  was treated with 25 equivalents of  $\text{Ph}_3\text{P}$  in  $\text{Me}_2\text{SO}$  solution. After 18 hours the system was examined by  $^{31}\text{P}$  NMR spectroscopy, which revealed that in excess of 20 equivalents of  $\text{Ph}_3\text{P}$  had been oxidized to  $\text{Ph}_3\text{PO}$ . In a parallel experiment, the reaction system was purged with  $\text{N}_2$  and the gas was passed into an aqueous  $\text{HgCl}_2$  solution, from which the known compound  $(\text{HgCl}_2)_3(\text{Me}_2\text{S})_2$  (41) precipitated. Greater than 95% of this compound, based on phosphine added, was recovered. No reaction occurs between  $\text{Ph}_3\text{P}$  and  $\text{Me}_2\text{SO}$  at  $\sim 190^\circ\text{C}$  for at least 1 hour (41). These observations are summarized in the catalytic cycle [22].



In further experiments *d*-biotin sulfoxide (25), a biological substrate (vide infra), was shown to be reduced in reaction [23] to *d*-biotin (26). The overall reaction involves a



sequence parallel to reactions [17] and [18], with  $K = 1.6 \times 10^4$  and  $k_1 = 1.4 \times 10^{-3} \text{ s}^{-1}$ . Catalytic turnover in a cycle analogous to [22] has not yet been investigated, but there is no apparent reason why 25 and 26 would not function in this respect.

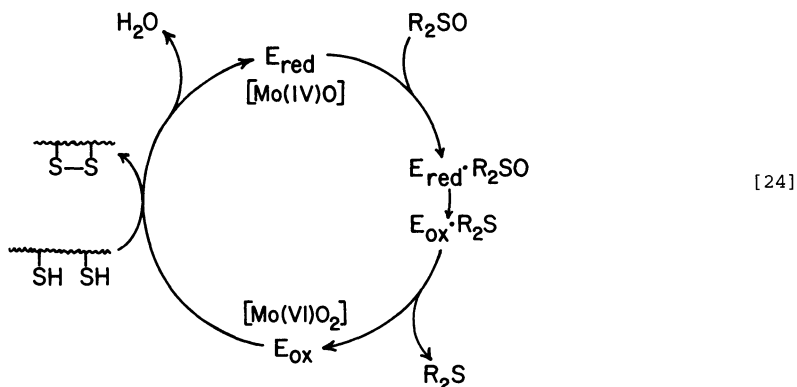
#### RELEVANCE TO ENZYMATIC REACTIONS

The reduction of sulfoxides by  $\text{MoO}(\text{L-NS}_2)(\text{DMF})$  is of particular significance in view of the discovery that d-biotin sulfoxide reductase from E. coli is a Mo-co dependent enzyme (42). The demonstration of a common cofactor for oxo-transfer molybdoenzymes (11-14) facilitates this conclusion, although at present the enzyme has not been extensively purified (43). Genetic studies have revealed that at least five genes are involved in the expression of d-biotin sulfoxide reductase activity (42,44). Moreover, four of these have been implicated in the expression of nitrate reductase activity. These genes appear to be involved in the synthesis or processing of the Mo-co required by nitrate reductase. A molybdenum requirement is further supported by the observation that the presence of tungstate in the growth medium sharply reduces the specific activity of the d-biotin sulfoxide reductase present (42), paralleling observations with other molybdoenzymes (45-47). Although further characterization of this enzyme is clearly necessary, its Mo-co dependence appears to be adequately substantiated.

d-Biotin sulfoxide reductase apparently functions to recover the vitamin d-biotin from its adventitious oxidation product 25. Enzymatic systems involved in the reduction of methionine sulfoxide to methionine have also been discovered and partially characterized (48-50). Inasmuch as the oxidation of Met residues in a number of proteins has been correlated with loss of biological activity and with several pathological conditions (51), including cataracts (52) and emphysema (53), these enzymes may be of considerable physiological importance. One enzyme, from E. coli, which acts on free methionine sulfoxide but apparently not on MetSO-containing peptides, has been purified to near-homogeneity (49). It is not known at present whether this or any of the other methionine sulfoxide reducing systems are molybdenum-dependent. The E. coli enzyme has an apparent molecular weight of 21,000 daltons and a maximum specific activity which corresponds to a turnover rate of  $1.6 \times 10^{-4} \text{ s}^{-1}$ , a rather small value for an enzymatic reaction. The saturation kinetics operative in model systems permit a direct comparison with enzymatic rates. Interestingly, the enzymatic rate is an order of magnitude slower than that of the model system with  $\text{Me}_2\text{SO}$  as the substrate. This indicates that Mo-based oxygen atom transfer chemistry can be kinetically competent for involvement in biological reactions. Dimethylsulfoxide is also reduced by a number of other organisms (54), ranging from bacteria to higher plants to animals, although this ability is not universal. In yeast this activity appears to be due to the methionine sulfoxide reducing systems present, inasmuch as methionine sulfoxide is a potent inhibitor of  $\text{Me}_2\text{S}$  product formation (55). The origin of reducing activity in other organisms remains to be characterized.

In this investigation, examples of the forward and reverse reactions [3] without detectable occurrence of the dimerization reaction [4] have been demonstrated. At this stage, reactions [16] and [23] and their associated kinetics features offer encouraging approaches to the Mo-mediated biological reduction of sulfoxides. The ability of  $\text{MoO}_2(\text{L-NS}_2)$  and  $\text{MoO}(\text{L-NS}_2)(\text{DMF})$  to transform other potential substrates by oxo-transfer reactions remains to be investigated. Several qualifications of the present results in the biological context are noted. The preceding reactions present one possibility for biological sulfoxide reduction -- direct oxygen atom transfer from substrate to reduced enzyme -- but other pathways, e.g., reductive oxygen removal to form water, are readily conceived. The extent to which the complexes  $\text{MoO}(\text{L-NS}_2)(\text{DMF})$  and  $\text{MoO}_2(\text{L-NS}_2)$  are reasonable structural models of the catalytic site of an enzyme such as d-biotin sulfoxide reductase can be assessed only after the enzyme has been thoroughly characterized. Development of the cycle [22] demonstrates that suitable coupling of oxo-transfer reactions effected by the foregoing complexes can result in catalysis. Obviously,  $\text{Ph}_3\text{P}$  is a non-physiological reductant. It and other tertiary phosphines have previously been shown to be catalytically oxidized in aerial systems containing dioxo-Mo(VI) complexes (56,57). In vivo, the source of electrons for reduction of sulfoxides appears to be thiol groups of cysteinyl-containing proteins. For methionine sulfoxide reductase in yeast, this protein is thioredoxin (58,59). For E. coli d-biotin sulfoxide reductase, a different heat-stable protein is involved which cannot be replaced by thioredoxin or glutaredoxin (43). In the case of E. coli methionine sulfoxide reductase, the thioredoxin system may be replaced in vitro by the artificial reductant dithioerythritol (52). The cycle [24] incorporates these observations in a suggested scheme for enzymatic reduction of sulfoxides. The relation between it and the cycle [22] is apparent. Allowance is made in cycle [24] for reduced substrate binding prior to release. More important is the inclusion of the reaction  $2\text{RSH} \rightarrow \text{RSSR} + 2\text{H}^+ + 2\text{e}^-$ . A more biologically realistic version of cycle [22] would include this couple as a reductant. Further research will involve attempted inclusion of dithiols in cycle [22] instead of phosphines, examination of the reaction of  $\text{MoO}(\text{L-NS}_2)(\text{DMF})$  and  $\text{MoO}_2(\text{L-NS}_2)$  with other potential substrates, and a study of the EPR spectra of Mo(V) complexes

(17 and others) to search for any relationships between spectral features of synthetic complexes and those of Mo(V) intermediates in enzymatic catalysis (7,8).



**Acknowledgement.** This research was supported by National Science Foundation Grant CHE 81-06017.

#### REFERENCES

1. L. E. Mortenson and R. N. F. Thorneley, *Ann. Rev. Biochem.* **48**, 387-418 (1979).
2. "Molybdenum and Molybdenum-Containing Enzymes," M. P. Coughlan, Ed., Pergamon Press, New York, 1980.
3. "Molybdenum Chemistry of Biological Significance," W. E. Newton and S. Otsuka, Ed., Plenum Press, New York, 1980.
4. "Current Perspectives in Nitrogen Fixation," A. H. Gibson and W. E. Newton, Ed., Elsevier/North-Holland, Inc., New York, 1981.
5. "Nitrogen Fixation, The Chemical-Biochemical-Genetic Interface," A. Müller and W. E. Newton, Ed., Plenum Press, New York, 1983.
6. M. J. Nelson, P. A. Lindahl, and W. H. Orme-Johnson, *Adv. Inorg. Biochem.* **4**, 1-40 (1982).
7. R. C. Bray, in "The Enzymes," Vol. XII, Part B, P. C. Boyer, Ed., Academic Press, New York, 1975, chapter 6.
8. R. C. Bray, *Adv. Enzymol.* **51**, 107-165 (1980).
9. B. K. Burgess and W. E. Newton, in ref. 5, pp. 83-110.
10. R. H. Holm, *Chem. Soc. Rev.* **10**, 455-490 (1981).
11. J. L. Johnson, in ref. 2, chapter 10.
12. J. L. Johnson, B. E. Hainline, and K. V. Rajagopalan, *J. Biol. Chem.* **255**, 1783-1786 (1980).
13. J. L. Johnson and K. V. Rajagopalan, *Proc. Natl. Acad. Sci. USA* **79**, 6856-6860 (1982).
14. K. V. Rajagopalan, J. L. Johnson, and B. E. Hainline, *Fed. Proc.* **41**, 2608-2612 (1982).  
R. C. Wahl, R. V. Hageman, and K. V. Rajagopalan, *Arch. Biochem. Biophys.* **230**, 264-273 (1984).  
J. L. Johnson, B. E. Hainline, K. V. Rajagopalan, and B. H. Arison, *J. Biol. Chem.* **259**, 5414-5422 (1984).
15. S. P. Cramer, R. Wahl, and K. V. Rajagopalan, *J. Am. Chem. Soc.* **103**, 7721-7727 (1981).
16. S. P. Cramer, L. P. Solomonson, M. W. W. Adams, and L. E. Mortenson, *J. Am. Chem. Soc.* **106**, 1467-1471 (1984).
17. J. Bordas, R. C. Bray, C. D. Garner, S. Gutteridge, and S. S. Hasnain, *Biochem. J.* **191**, 499-508 (1980).
18. J. A. Pateman, D. J. Cove, B. M. Rever, and D. B. Roberts, *Nature* **201**, 58-60 (1964).
19. A. Nason, K.-Y. Lee, S. S. Pan, P. A. Ketchum, A. Lamberti, and J. DeVries, *Proc. Natl. Acad. Sci. USA* **68**, 3242-3246 (1971).
20. J. L. Johnson, H. P. Jones, and K. V. Rajagopalan, *J. Biol. Chem.* **252**, 4994-5003 (1977).
21. P. T. Pienkos, V. K. Shah, and W. J. Brill, *Proc. Natl. Acad. Sci. USA* **74**, 5468-5471 (1977).
22. J. T. Spence, *Coord. Chem. Rev.* **48**, 59-82 (1983).
23. J. M. Berg, K. O. Hodgson, S. P. Cramer, J. L. Corbin, A. Elsberry, N. Pariyadath, and E. I. Stiefel, *J. Am. Chem. Soc.* **101**, 2774-2776 (1979).  
E. I. Stiefel, K. F. Miller, A. E. Bruce, J. L. Corbin, J. M. Berg, and K. O. Hodgson, *ibid.* **102**, 3624-3626 (1980).
24. A. Bruce, J. L. Corbin, P. L. Dahlstrom, J. R. Hyde, M. Minelli, E. I. Stiefel, J. T. Spence, and J. Zubieta, *Inorg. Chem.* **21**, 917-926 (1982).
25. J. M. Berg and R. H. Holm, *Inorg. Chem.* **22**, 1768-1771 (1983).
26. O. A. Rajan, J. T. Spence, C. Lemon, M. Minelli, M. Sato, J. H. Enemark, P. M. H. Kroneck, and K. Sulger, *Inorg. Chem.* **22**, 3065-3072 (1983).
27. I. Buchanan, M. Minelli, M. T. Ashby, T. J. King, J. H. Enemark, and C. D. Garner, *Inorg. Chem.* **23**, 495-500 (1984).
28. P. Subramian, B. Kaul, and J. T. Spence, *J. Mol. Catal.* **23**, 163-177 (1984).

29. J. M. Berg and R. H. Holm, J. Am. Chem. Soc. **106**, in press.
30. M. S. Reynolds, J. M. Berg, and R. H. Holm, Inorg. Chem. **23**, in press.
31. G. J.-J. Chen, J. W. McDonald, and W. E. Newton, Inorg. Chem. **15**, 2612-2615 (1976).
32. T. Matsuda, K. Tanaka, and T. Tanaka, Inorg. Chem. **18**, 454-457 (1979).
33. P. C. H. Mitchell and R. Scarle, J. Chem. Soc., Dalton Trans., 2552-2555 (1975).
34. E. I. Stiefel, Prog. Inorg. Chem. **22**, 1-223 (1977).
35. K. Tatsumi and R. Hoffmann, Inorg. Chem. **19**, 2656-2658 (1980).
36. M. Gullotti, A. Pasini, G. M. Zanderighi, G. Ciani, and A. Sironi, J. Chem. Soc., Dalton Trans., 902-908 (1981). A. Chiesi Villa, L. Coghi, A. G. Manfredotti, and C. Guastini, Cryst. Struct. Commun. **3**, 551-554 (1974).
37. R. J. Butcher, B. R. Penfold, and E. Sinn, J. Chem. Soc., Dalton Trans., 668-675 (1979).
38. J. L. Johnson and K. V. Rajagopalan, J. Biol. Chem. **252**, 2017-2025 (1977).
39. I. Buchanan, M. Minelli, M. T. Ashby, T. J. King, J. H. Enemark, and C. D. Garner, Inorg. Chem. **23**, 495-500 (1984).
40. J. Topich and J. T. Lyon, III, Polyhedron **3**, 55-60, 61-65 (1984).
41. H. E. Szmant and O. Cox, J. Org. Chem. **31**, 1595-1598 (1966).
42. A. del Campillo-Campbell and A. Campbell, J. Bacteriol. **149**, 469-478 (1982).
43. A. del Campillo-Campbell, D. Dykhuizen, and P. P. Cleary, Meth. Enzymol. **62**, 379-385 (1979).
44. D. Dykhuizen, J. Bacteriol. **115**, 662-667 (1973).
45. K.-Y. Lee, R. Erickson, S.-S. Pan, G. Jones, F. May, and A. Nason, J. Biol. Chem. **249**, 3953-3959 (1974).
46. J. L. Johnson, K. V. Rajagopalan, and H. J. Cohen, J. Biol. Chem. **249**, 859-866 (1974).
47. R. H. Scott, G. T. Sperl, and J. A. DeMoss, J. Bacteriol. **137**, 719-726 (1979).
48. S. Black, E. M. Harte, B. Hudson, and L. Wartofsky, J. Biol. Chem. **235**, 2910-2916 (1960).
49. S. Ejiri, H. Weissbach, and N. Brot, Anal. Biochem. **102**, 393-398 (1980).
50. N. Brot, L. Weissbach, J. Werth, and H. Weissbach, Proc. Natl. Acad. Sci. USA **78**, 2155-2158 (1981).
51. N. Brot and H. Weissbach, Trends Biochem. Sci. **7**, 137-139 (1982).
52. M. H. Garner and A. Spector, Proc. Natl. Acad. Sci. USA **77**, 1274-1277 (1980).
53. H. Carp, F. Miller, J. R. Hoidal, and A. Janoff, Proc. Natl. Acad. Sci. USA **79**, 2041-2045 (1982).
54. S. H. Zinder and T. D. Brock, J. Gen. Microbiol. **105**, 335-342 (1978).
55. B. J. Anness, C. W. Banforth, and T. Wainwright, J. Inst. Brew. **85**, 346-349 (1979).
56. R. Barral, C. Bocard, I. Sérée de Roch, and L. Sajus, Tetrahedron Lett., 1693-1696 (1972); Kinet. Catal. **14**, 130-133 (1973).
57. G. Speier, Inorg. Chim. Acta **33**, 139-141 (1979). J. Deli and G. Speier, Transition Met. Chem. **6**, 227-229 (1981).
58. P. G. Porqué, A. Baldesten, and P. Reichard, J. Biol. Chem. **245**, 2371-2374 (1970).
59. A. Holmgren, Trends Biochem. Sci. **6**, 26-29 (1981).